Chapter 5

Dielectric and Mechanical properties of La doped $CaCu_3Ti_4O_{12}$/ Poly(vinylidene fluoride) Composites

Structural, dielectric and mechanical properties of La doped $CaCu_3Ti_4O_{12}$ / PVDF composites are described in this chapter. La doped $CaCu_3Ti_4O_{12}$ (LaCCTO) has been prepared by semi wet method. La doping in CCTO results in considerable improvement in the dielectric properties of CCTO. LaCCTO dispersed PVDF (PVDF-LaC) composites have been prepared by melt extrusion method. LaCCTO dispersion in PVDF improves the thermal, dielectric as well as mechanical properties of PVDF-LaC composites.

5. Results and discussion

5.1. Structural Analysis

X-ray diffraction patterns of LaCCTO, PVDF and the composites containing 10, 20 and 50 wt % LaCCTO (PVDF-LaC) are shown in Fig 5.1. Formation of the single phase solid solution in LaCCTO is confirmed by powder X-ray diffraction (XRD) using CuKα radiation. In the case of LaCCTO, the diffraction peaks corresponding to the planes (220), (310), (222), (321), (400), (422) and (440) of CCTO are observed at 2θ values of 34.2°, 38.5°, 42.3°, 45.8°, 49.2°, 61.3° and 72.2° respectively. This confirms the formation of single phase [Sinclair et al (2002)]. There is no evidence of presence of any secondary phase in LaCCTO. Lattice parameter "a" increases from 7.3907 Å (for CCTO) to 7.3918 Å for LaCCTO. This is due to larger ionic radius of La^{3+} (1.15 Å) as compared to Ca^{2+} (1.05Å) [Shannon and Prewitt (1970)].

α- PVDF has been used in the present work (as supplied). This is proved by its characteristic 2θ peaks at 17.7°, 18.7°and 19.9° corresponding to (100), (020) and (110) reflections respectively [Varma et al (2010)]. Intensity of three major peaks (220), (400) and (422) in the composites increases with increasing content of LaCCTO. Predominance

of LaCCTO phase can be seen in PVDF-50LaC. This is indicated by the suppression of the peaks of PVDF.

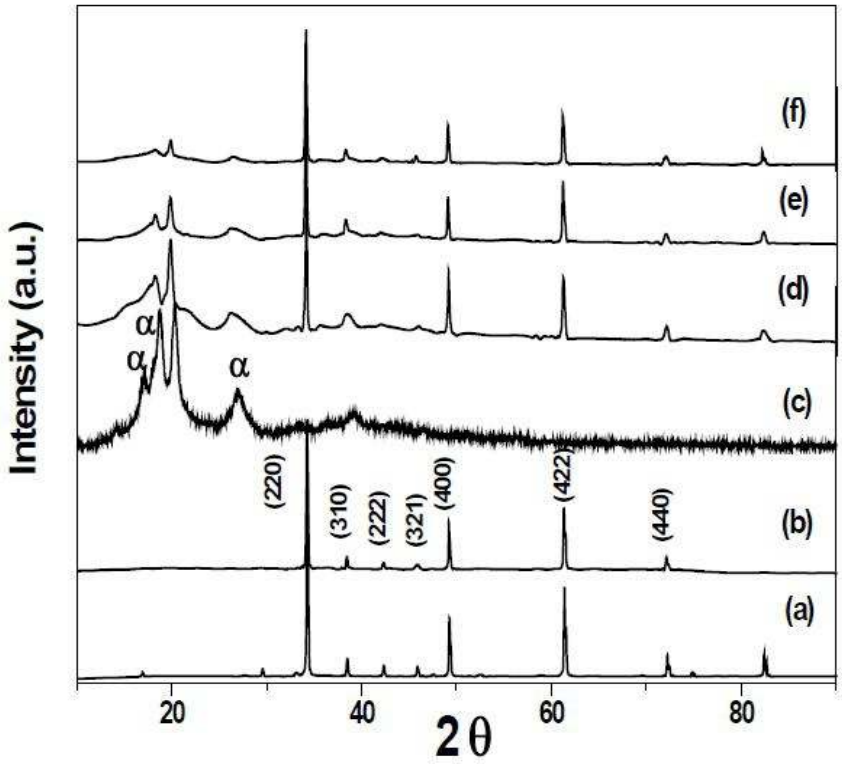

Figure 5.1 X-ray diffraction patterns for (a) CCTO, (b) LaCCTO, (c) PVDF, (d) PVDF-10LaC, (e) PVDF-20LaC and (f) PVDF-50LaC composites.

5.2. Surface morphology

Figure 5.2 shows SEM micrographs of PVDF and the composites. Pure PVDF has spherulitic morphology. Distribution of ceramic particles in the polymer matrix is very important factor in determining the resulting properties. It is found that the spherulitic morphology of pure PVDF is significantly changed by the dispersion of LaCCTO powder. At low content of the filler, particles are well distributed but at high content, the ceramic network forms. This is evident from the SEM micrograph of the PVDF-50LaC composite. These changes in the morphology of the composites influence the properties.

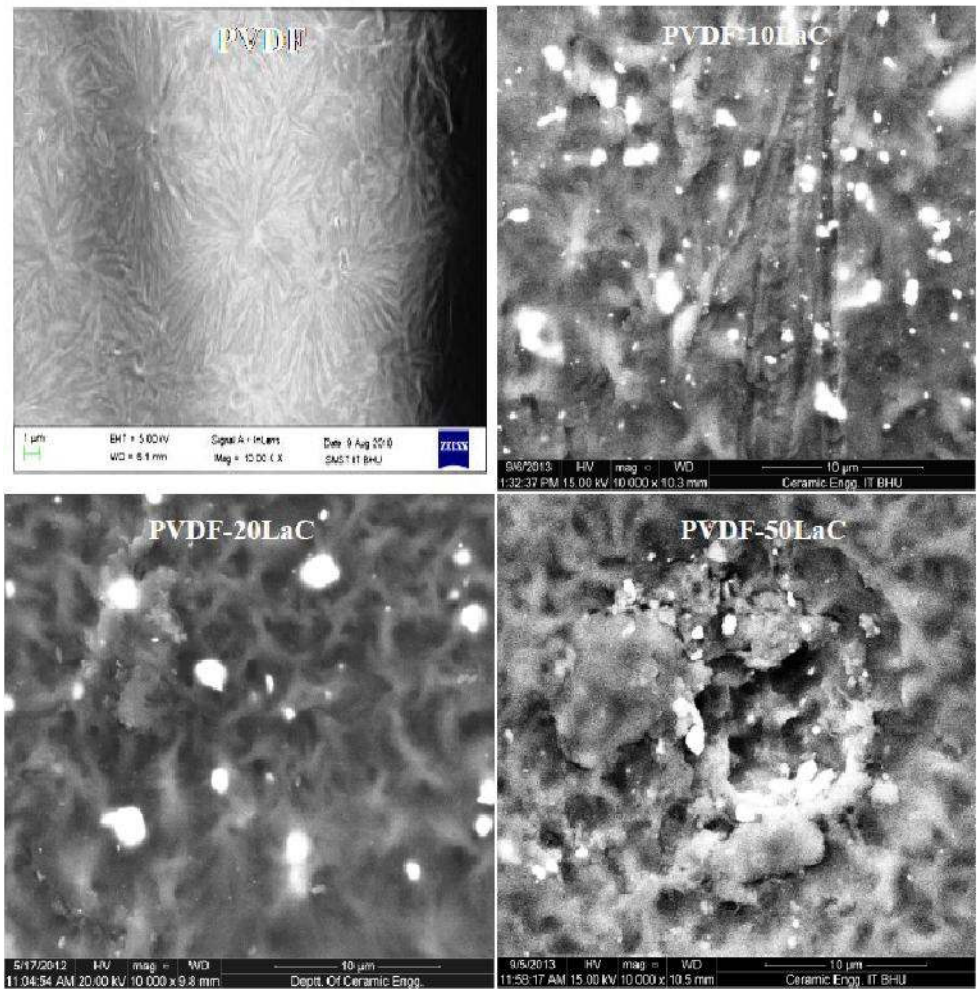

Figure 5.2 Scanning electron micrographs of PVDF, PVDF-10LaC, PVDF-20LaC and PVDF-50LaC composites.

5.3. Thermal behavior

Thermogravimetric analysis (TGA) has been carried out to study the thermal stability of the polymer and the composites. Thermograms recorded for the pure PVDF and its composites are shown in Fig 5.3. It is observed that pure PVDF is stable up to 400°C and complete degradation of the polymer occurs at around 500°C. Addition of the filler alters the thermal decomposition behaviour of PVDF. The degradation temperature shifts to higher temperature side i.e. from 442^{0}C in PVDF to 444^{0}C, 458^{0}C and 473^{0}C for PVDF-

10LaC, PVDF-20LaC and PVDF-50LaC respectively. It shows that LaCCTO dispersion improves the thermal stability of the composites.

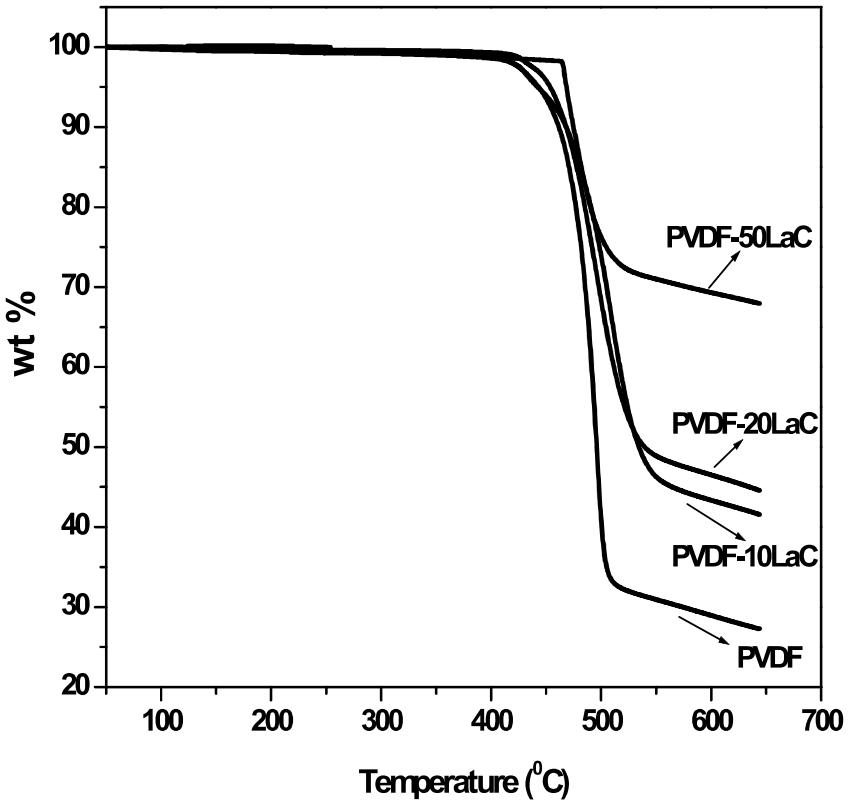

Figure 5.3 TGA of pure PVDF, PVDF-10LaC, PVDF-20LaC and PVDF-50LaC composites.

5.4. Mechanical properties

Figure 5.4(a) shows the stress-strain curves of PVDF and the composites. Three samples are tested for each composition and the average is taken. Considerable increase is observed in the value of Young's modulus which is calculated from the slope of the linear portion of the plots. For PVDF, PVDF-10LaC, PVDF-20LaC and PVDF-50LaC, Young's modulus is 750, 840, 1260, 1450 MPa, respectively (Fig 5.4 b). Elongation at the breaking point decreases from 30% in PVDF to 17%, 16% and 15% in PVDF-10LaC, PVDF-20LaC and PVDF-50LaC composites respectively (Fig 5.4 c). This increase in the Young's modulus with filler content can be attributed to increase in the resistance to the

free movement of the polymeric chains by much harder ceramic particles. This is also a reason for decrease in elongation at the breaking point with increasing concentration of ceramic in the PVDF matrix.

(a)

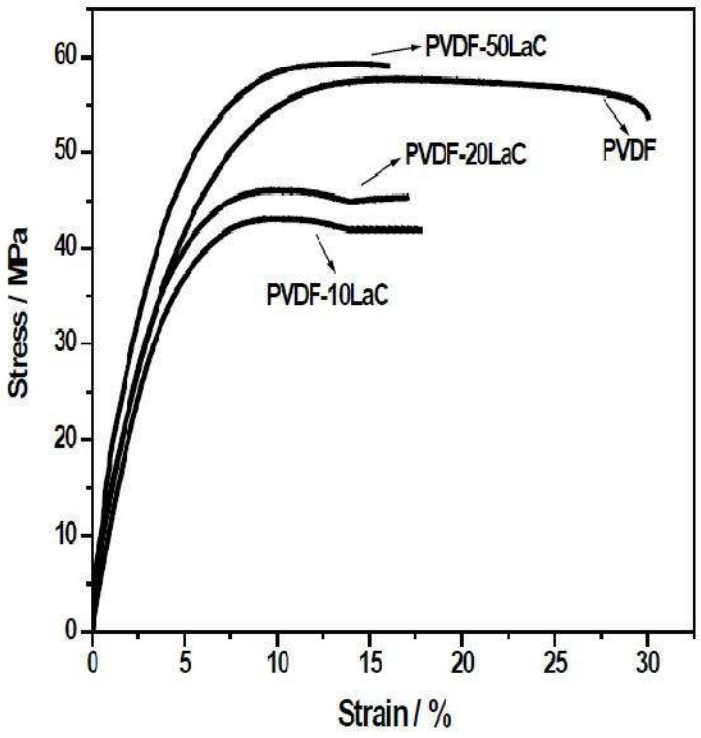

Figure 5.4 (a) Stress-strain curves for pure PVDF, PVDF-10LaC, PVDF-20LaC and PVDF-50LaC composites

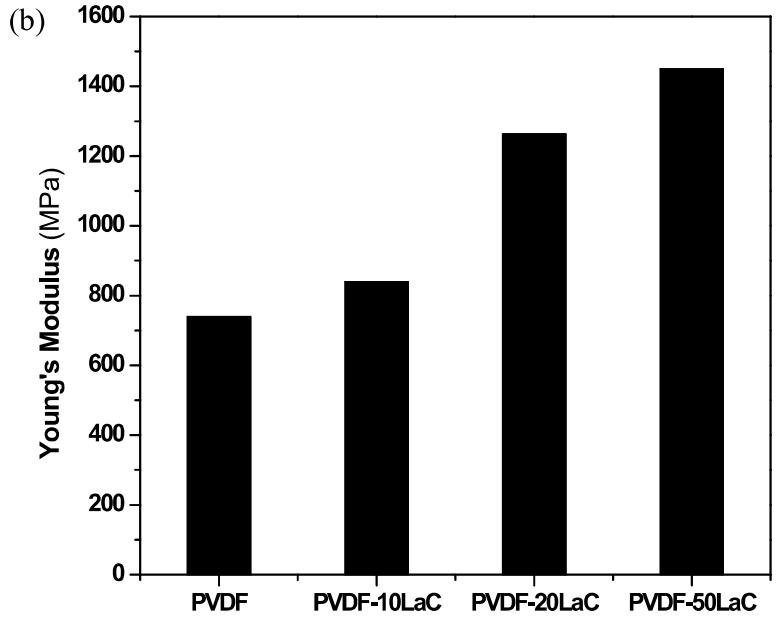

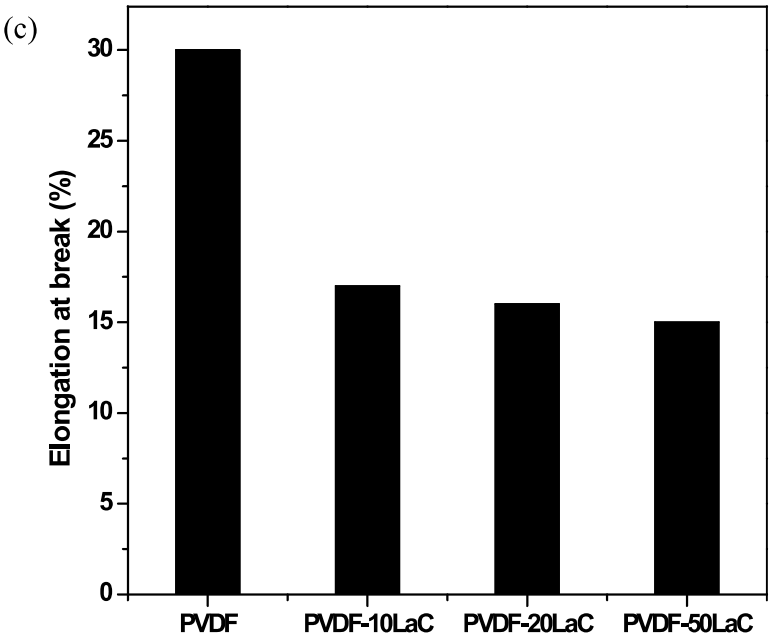

Figure 5.4(b) Young's modulus of PVDF and the composites, (c) Elongation at the breaking point of PVDF and the composites.

5.5. Dielectric properties

Frequency dependence of ε' of CCTO, LaCCTO, PVDF and the composites at 40^0C is shown in figs 5.5 (a and e). At 40°C and 100 Hz, ε' of CCTO and LaCCTO is 3100 and 8850 respectively. ε' of CCTO and LaCCTO decreases rapidly with increase in frequency upto a particular frequency and thereafter it becomes almost independent of frequency. The frequency after which it becomes constant is lower in LaCCTO than that in CCTO. The intrinsic dielectric response in CCTO and LaCCTO is due to barrier layer capacitance associated with grains-grain boundaries interfaces. The giant permittivity depends on the microstructure and on the formation of the internal boundary layer capacitors (IBLC) between the grains [Sinclair et al (2002)]. Doping CCTO with La significantly modifies the grain boundaries leading to more efficient IBLCs. ε' increases with temperature in PVDF, it is 3 at 40^0C and 100 Hz which increases to 8 at 120^0C and 100 Hz (Fig 5.5 c). Dielectric permittivity increases with increasing content of LaCCTO in PVDF at frequencies above 10 Hz (Fig 5.5 e). Values of dielectric permittivity at 40^0C and 100 Hz for PVDF, PVDF-10LaC, PVDF-20LaC and PVDF-50LaC are 3, 13, 24 and 60 respectively (Fig 5.5 e). PVDF is present in α phase, which is non-polar. Due to the non-polar nature of PVDF, ε' is low for PVDF. Dielectric permittivity decreases with increase in frequency upto a particular frequency and thereafter it becomes constant (Figs 5.5 g, i and k). The frequency beyond which it becomes constant shifts to higher value with increasing temperature. The high-ε' of the composites is mainly because of interfacial polarization and high dielectric permittivity of the ceramic filler used. Interfacial polarization is always present in these composites due to difference in the conductivity between the matrix and the dispersed phase (LaCCTO in this case). It is important to note that dielectric permittivity does not change much over the frequency range, 10^2-10^6 Hz. It is a desirable feature for use of these materials in devices.

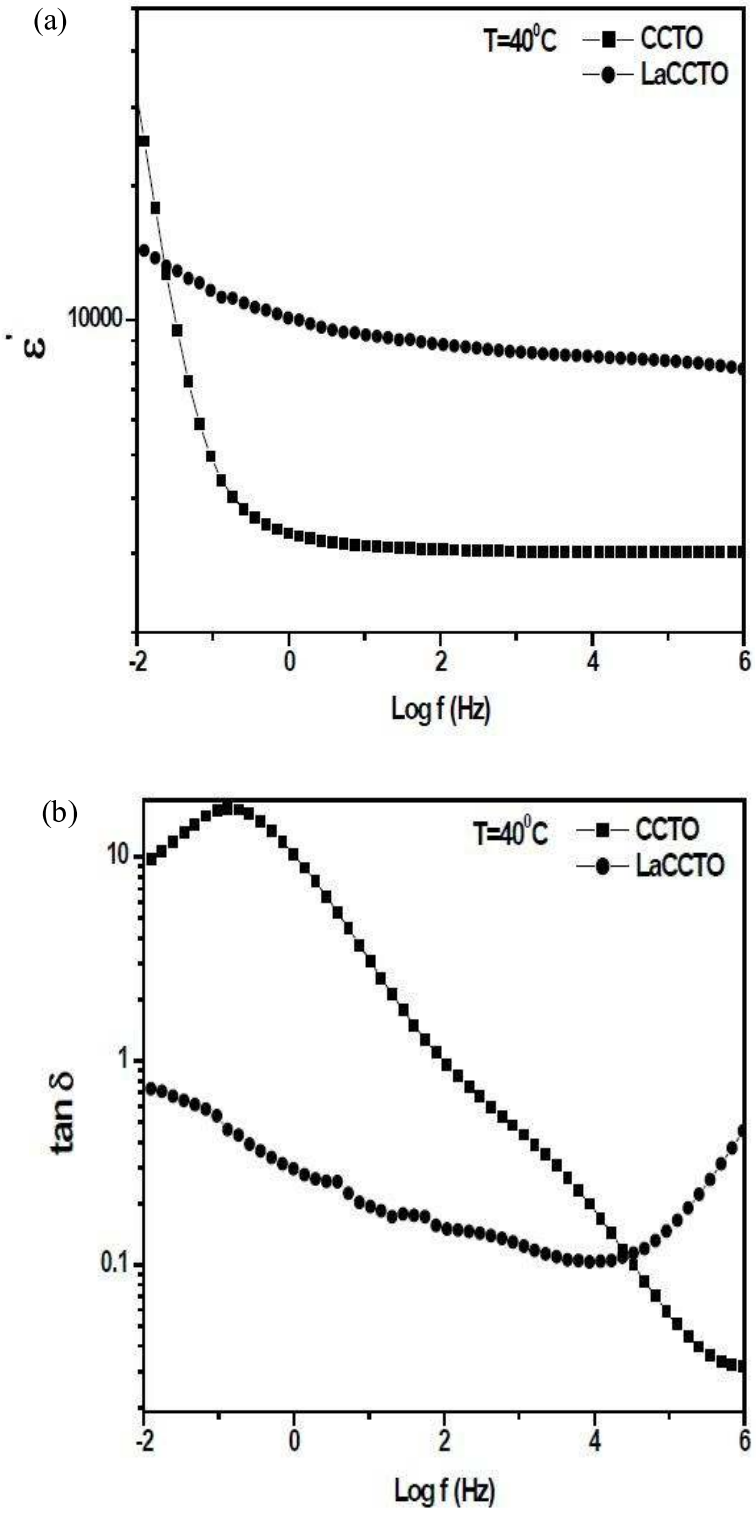

Figure 5.5 Frequency dependence of dielectric permittivity and tan δ (a and b) of CCTO and LaCCTO at 40^0C

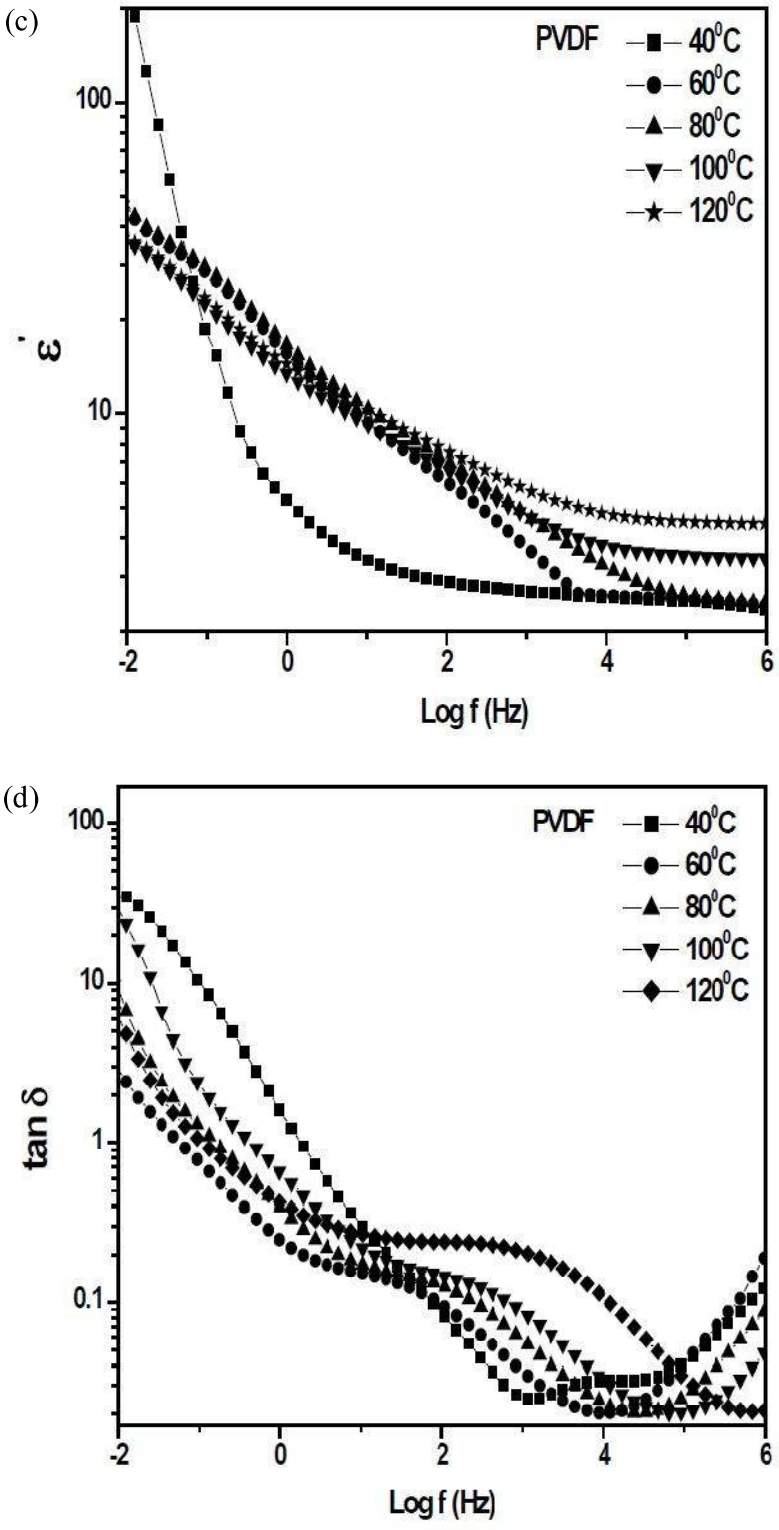

Figure 5.5 Frequency dependence of dielectric permittivity and tan δ (c and d) of PVDF at different temperatures.

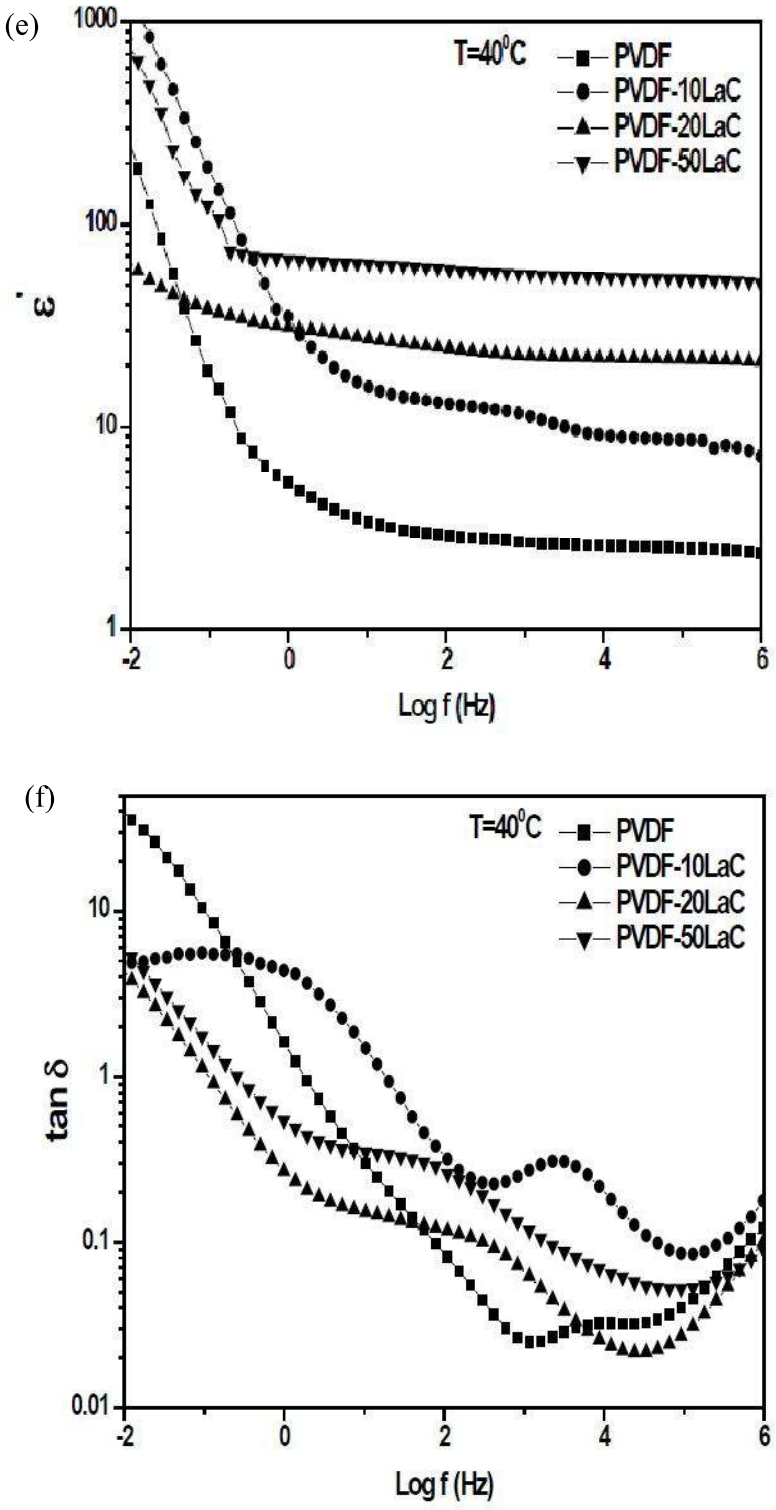

Figure 5.5 Frequency dependence of dielectric permittivity and tan δ (e and f) of PVDF and all the composites at 40^0 C

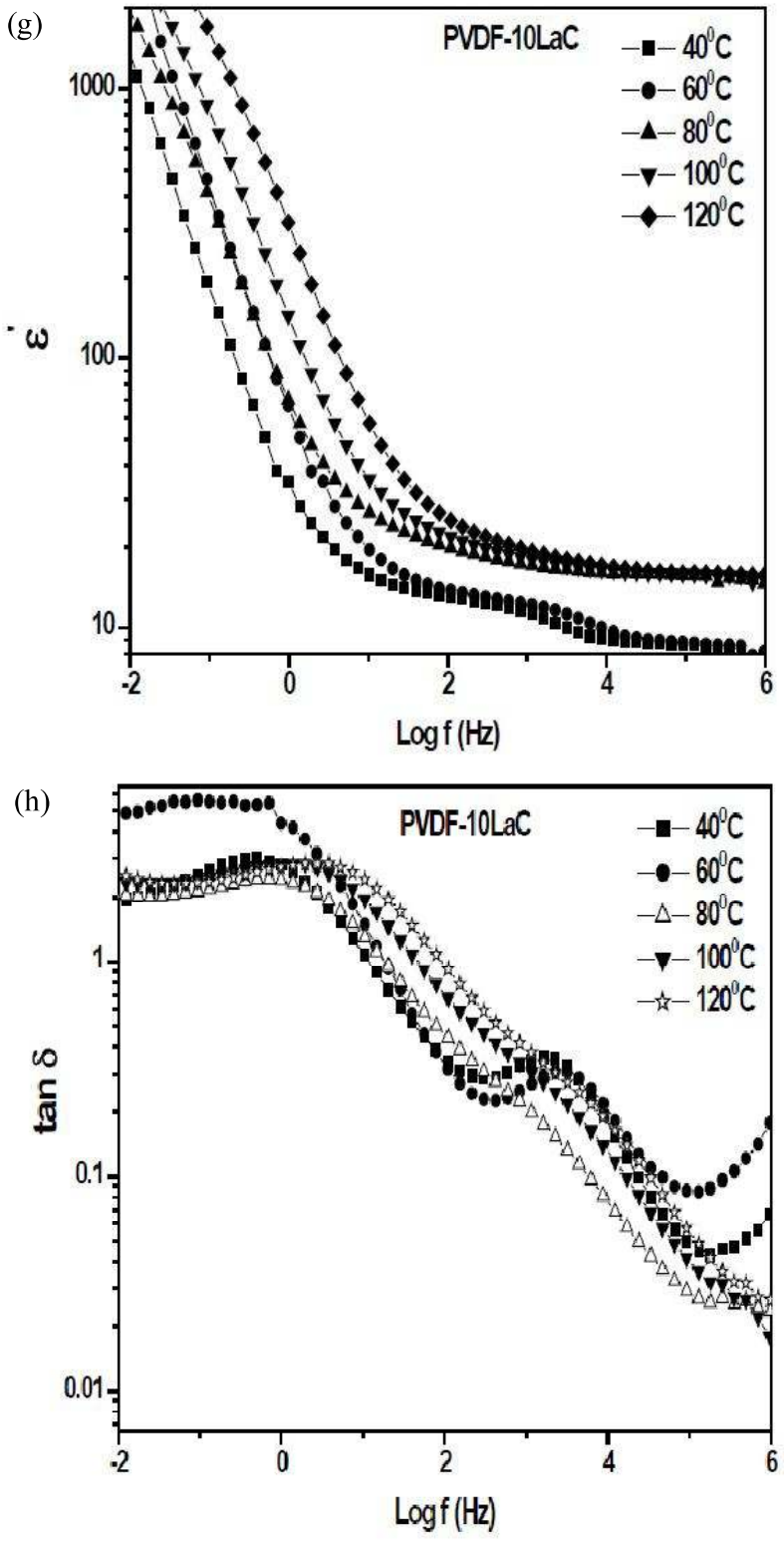

Figure 5.5 Frequency dependence of dielectric permittivity and tan δ (g and h) of PVDF-10LaC at different temperatures

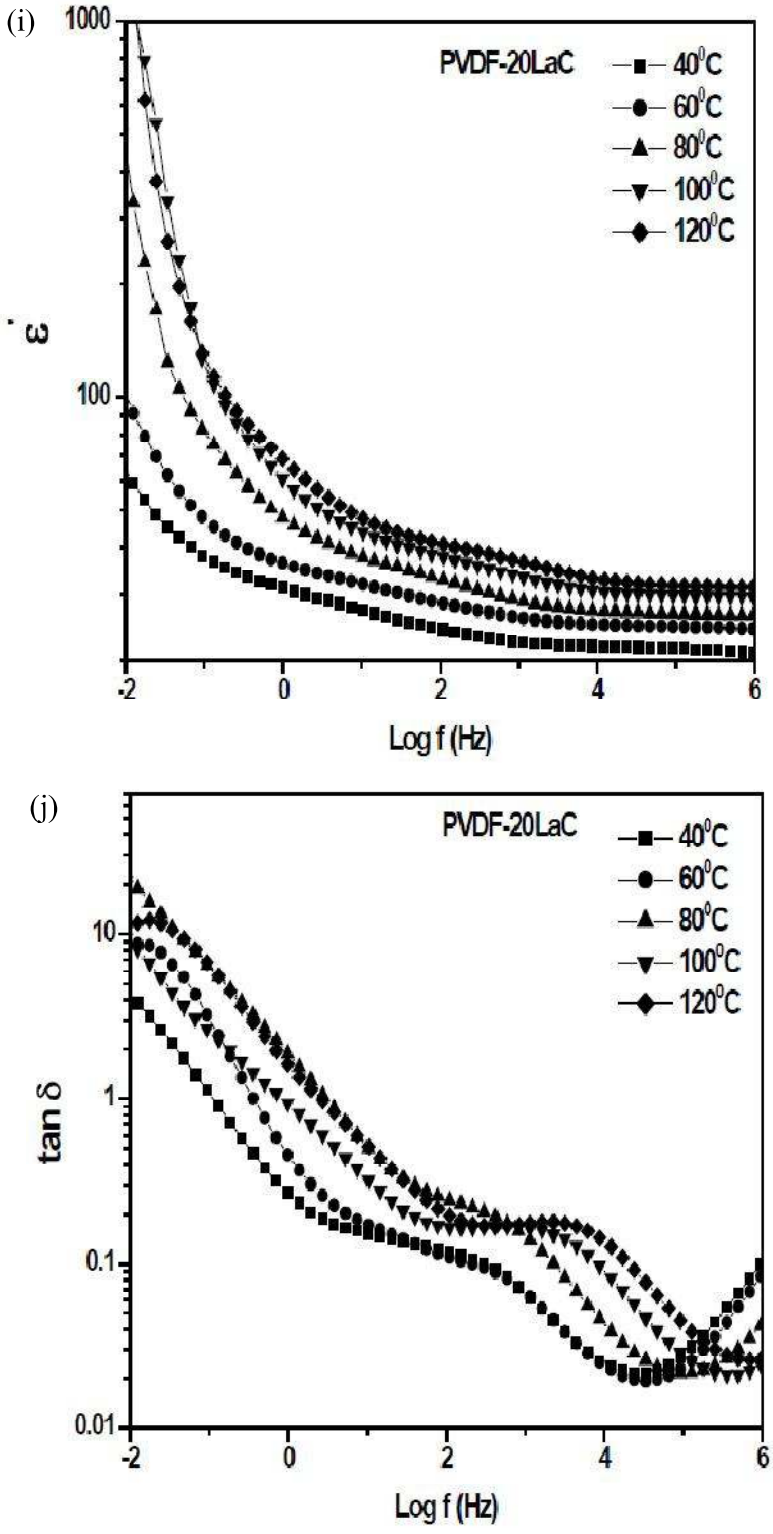

Figure 5.5 Frequency dependence of dielectric permittivity and tan δ (i and j) of PVDF-20LaC at different temperatures

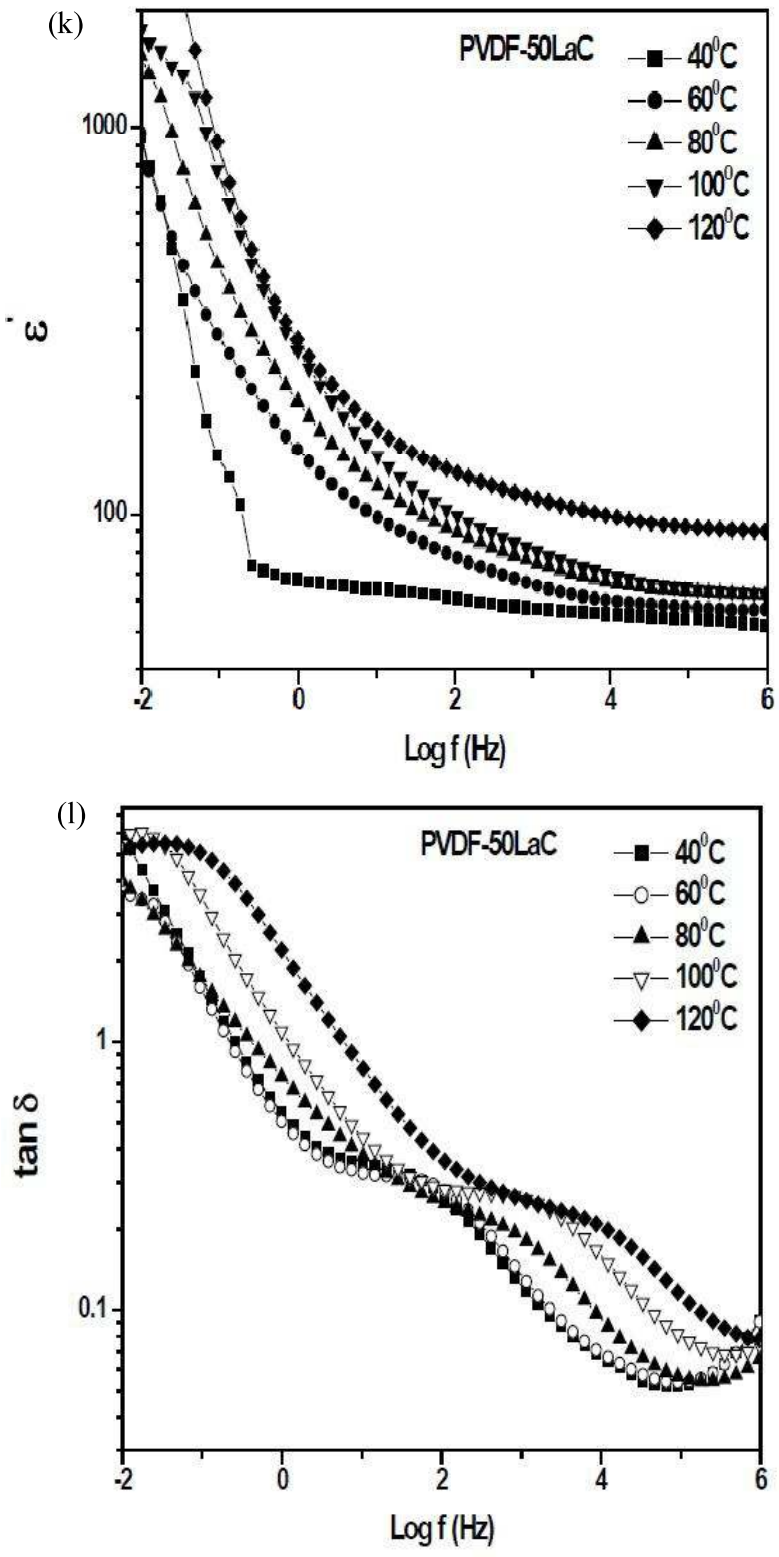

Figure 5.5 Frequency dependence of dielectric permittivity and tan δ (k and l) of PVDF-50LaC at different temperatures.

Frequency dependence of dielectric loss, (tan δ) of CCTO, LaCCTO, PVDF and all the composite samples at 40^0C is shown in Figs 5.5 (b and f). On doping with La, considerable decrease in the dielectric loss has been observed. Value of dielectric loss of CCTO at 40° C and 100 Hz is 0.86 which decreases to 0.13 in LaCCTO (Fig 5.5 b). The dielectric loss at 40°C and 100Hz for PVDF, PVDF-10LaC, PVDF-20LaC and PVDF-50LaC is 0.08, 0.33, 0.21 and 0.34 respectively (Fig 5.5 f).

In the case of PVDF-LaC composites, one relaxation appears in the lower frequency range (10^{-2}-1 Hz) and other appears in the intermediate frequency range (within 10^3- 10^5) depending upon composition and temperature (Figs 5.5 h, j and l). A low frequency relaxation becomes clearly visible at high temperature. Relaxation at lower frequency is attributed to Maxwell Wagner polarization in the composites and the one in the higher frequency range is due to α_c relaxation associated with molecular motion of the polymer chains in the crystalline regions of PVDF. The glass transition relaxation α_a of PVDF occurs beyond 1 MHz, beyond the frequency range of our measurement (Fig 5.5 d) [Gregoria and Cestari (1994); Gregoria and Ueno (1999); Channel and Jog (2008)]. These relaxation peaks shift to higher frequency with increase in temperature, indicating lower relaxation time (τ). This seems to be due to the ease of relaxation because of decreasing viscosity of the polymer with temperature.

To understand the nature of dielectric relaxation, use is made of modulus spectroscopy. Electrical modulus is defined as inverse of the complex permittivity.

$$M^* = \frac{1}{\varepsilon^*} = \frac{1}{(\varepsilon' - J\varepsilon'')} = \frac{\varepsilon'}{(\varepsilon'^2 + \varepsilon''^2)} + \frac{J\varepsilon''}{(\varepsilon'^2 + \varepsilon''^2)} = M' + J.M'' \qquad (5.1)$$

where M', ε', and M", ε" are the real and the imaginary parts of the modulus and permittivity respectively. M' decreases on dispersing LaCCTO in the PVDF matrix (Fig 5.6 a). This decrease in M' shows that ε' increases with the ceramic reinforcement. Variation of M'' with temperature for PVDF is shown in fig 5.6 (b). Fig 5.6 (c) shows the variation of imaginary part of electrical modulus (M") at 40^0C as a function of frequency

for PVDF and all the composite samples. A relaxation peak is present in PVDF as well as in the composites at intermediate frequency. This relaxation is due to α_c relaxation associated with the molecular motion of the polymer chains in the crystalline regions of PVDF as mentioned above. It is observed that this relaxation peak shifts to lower frequency in the composites with increase in the CCTO content. This is due to restricted mobility of the polymeric chains because of their interaction with the stiff filler particles. It is also evident from the Fig 5.7 (c) that with ceramic dispersion in PVDF matrix, the maximum value of M" decreases. This shows that the dielectric permittivity as well as the dielectric loss is more in the composites as compared to that in the pure PVDF.

Figures 5.6 (d-f) show variation of M" vs log f for PVDF-LaC composites at different temperatures. In PVDF-10LaC and PVDF-50LaC, it is observed that another peak appears in the low frequency range at high temperature. This peak is not observed at 40^{o}C, as it is present at much lower frequency. In PVDF-20LaC, this low frequency relaxation is not observed even at high temperature. Reason for this is not clear at present. It is not observed in PVDF also. Therefore, this relaxation is attributed to Maxwell-Wagner-Sillar (MWS) polarization [Ramajo et al (2008); Hedvig (1977)]. Maxwell Wagner Sillar polarization is always present in the multiphase systems having phases with different conductivities i.e. electrical heterogeneities. In such materials, the charge accumulates at the ceramic particles - polymer interface. This gives rise to space charge polarization which gives high value of dielectric permittivity as well as the dielectric loss. As the dielectric permittivity of LaCCTO is much higher than that of PVDF matrix, unbounded charges form the large dipoles at the polymer matrix – ceramic interface. These induced dipoles find it difficult to follow the alternation of the electric field and thus the resulting relaxation process occurs in the low frequency region or at high temperatures. It is observed that with increase in temperature, α_c relaxation as well as MWS relaxation shifts to higher frequency.

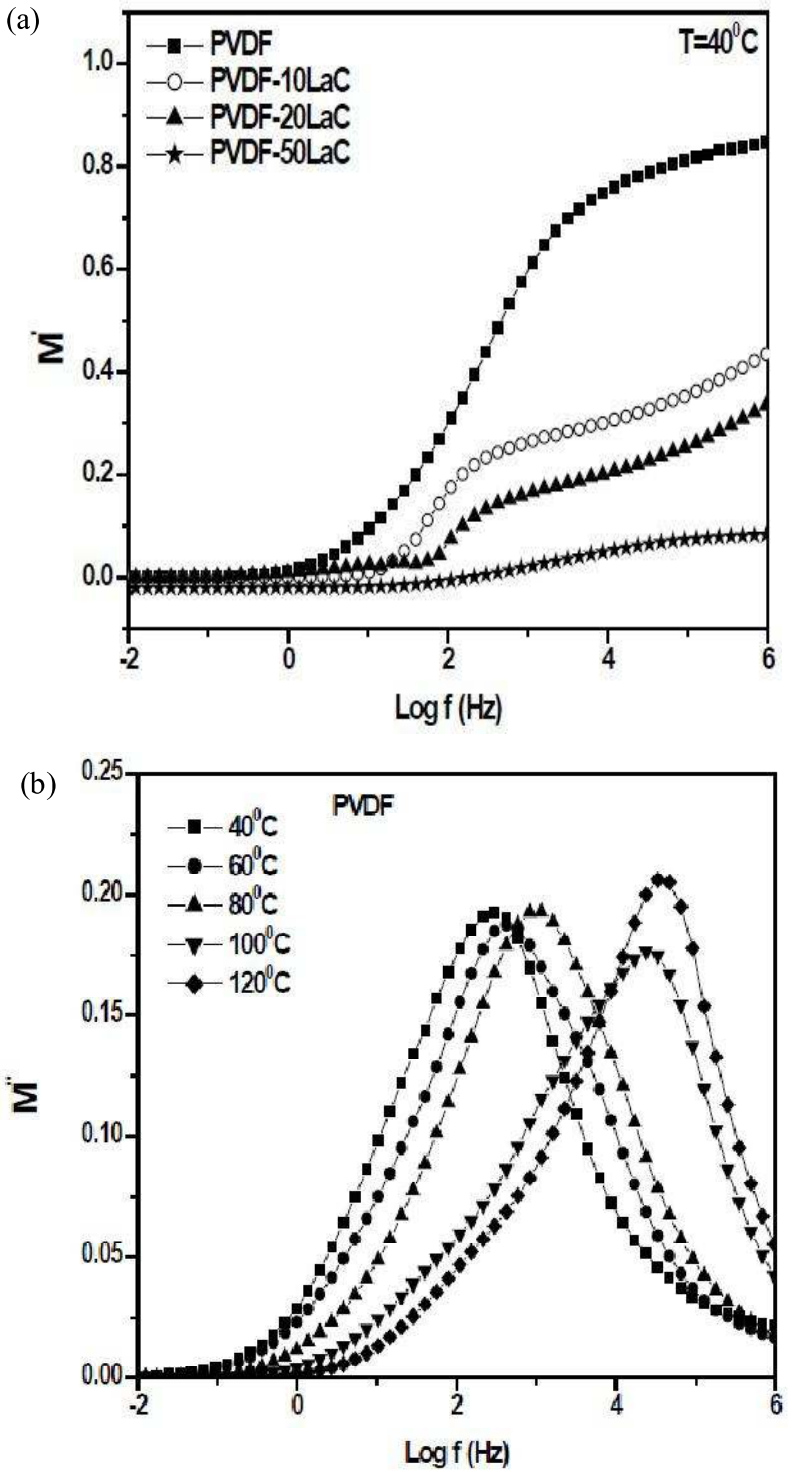

Figure 5.6 (a) M' vs log f plots of PVDF and composites at 40^0 C, M'' vs log f plots of (b) PVDF at different temperatures

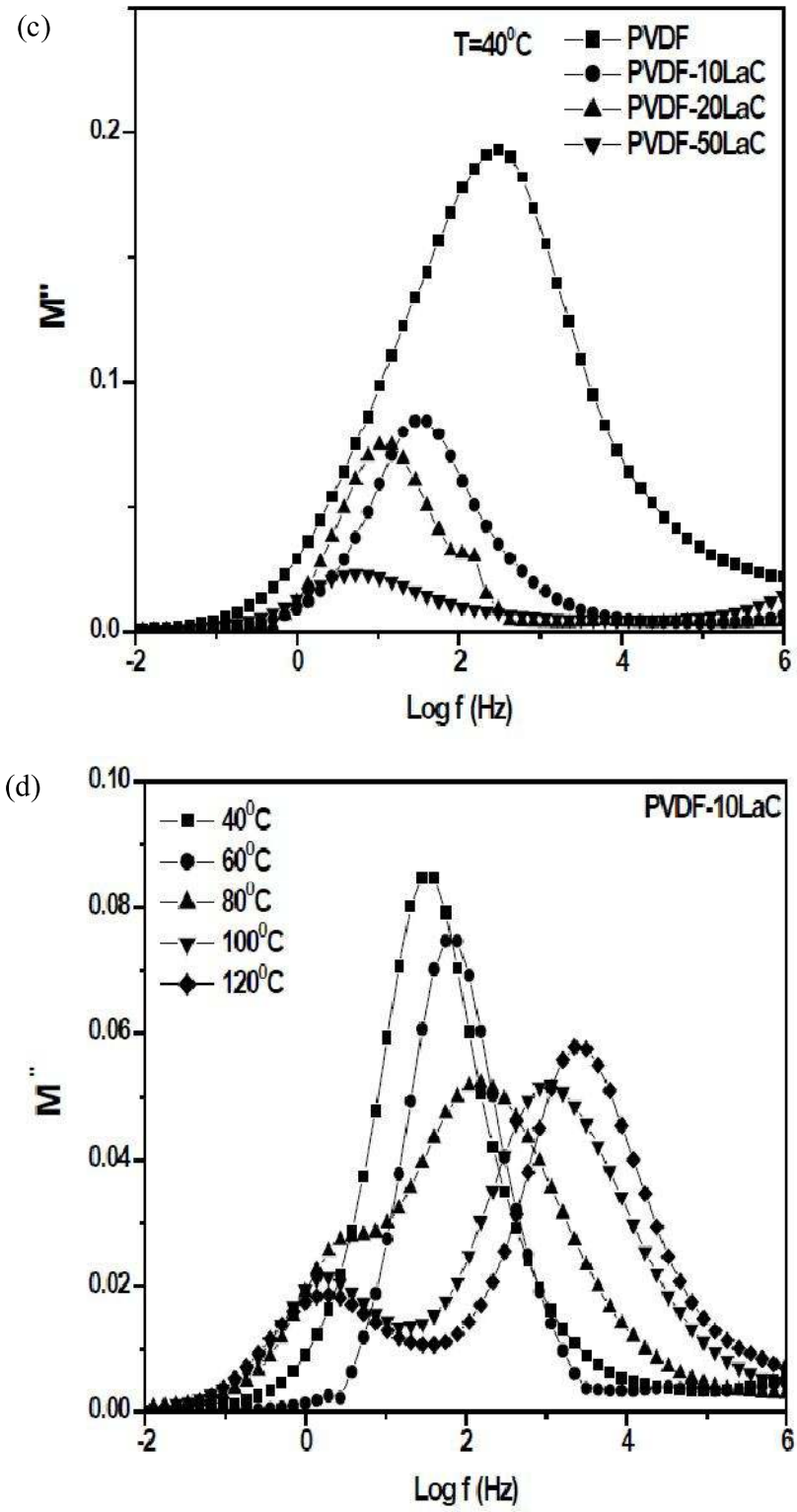

Figure 5.6 M" vs log f plots of (c) PVDF and PVDF-LaC composites at 40^0C, (d) PVDF-10LaC at different temperatures

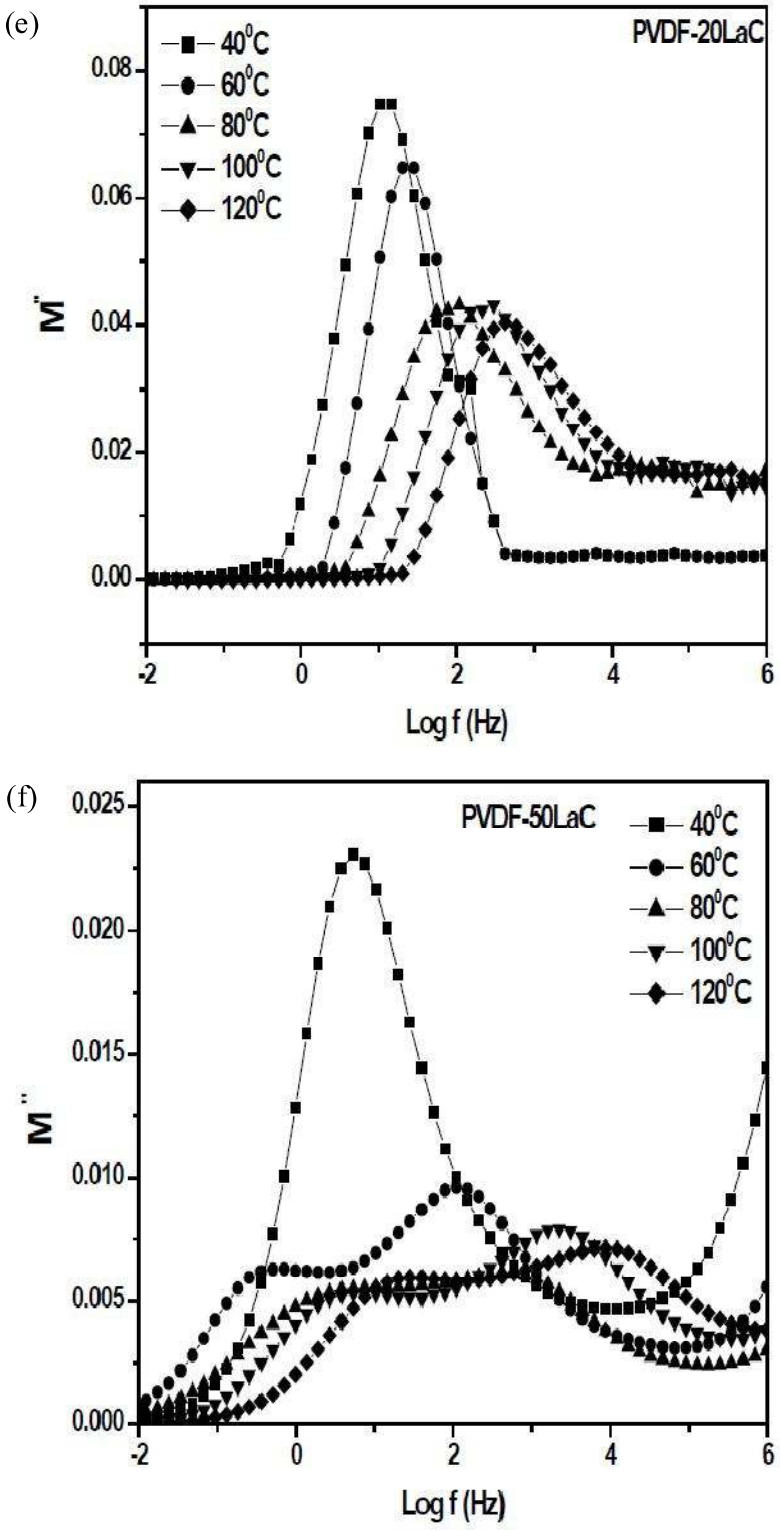

Figure 5.6 M" vs log f plots of (e) PVDF-20LaC at different temperatures, (f) PVDF-50LaC at different temperatures.

Relaxation times, τ was determined using the relation $\tau = \frac{1}{2\pi f}$ where f is the frequency in cycles per second at the peak position in M" vs log f plots for the higher frequency peak. Plots of log τ vs 1000/T for LaCCTO, PVDF, PVDF-10LaC, PVDF-20LaC and PVDF-50LaC are shown in Fig 5.7. These plots are linear in accordance with Arrhenius relationship given below.

$$\tau_{max} = \tau_o \exp(\frac{E_R}{kT}) \qquad (5.2)$$

where E_R is the activation energy associated with the relaxation process, τ_o the pre-exponential factor, k is the Boltzmann constant and T is the absolute temperature. Activation energy obtained from the slopes of these linear plots for various samples is given in Table 5.1. It is observed that the activation energy E_R for the α_c relaxation increases with increasing content of LaCCTO. This is due to increase in the stiffness of the composites with increasing content of LaCCTO which makes the movement of the polymeric chains difficult in the crystalline regions as mentioned above.

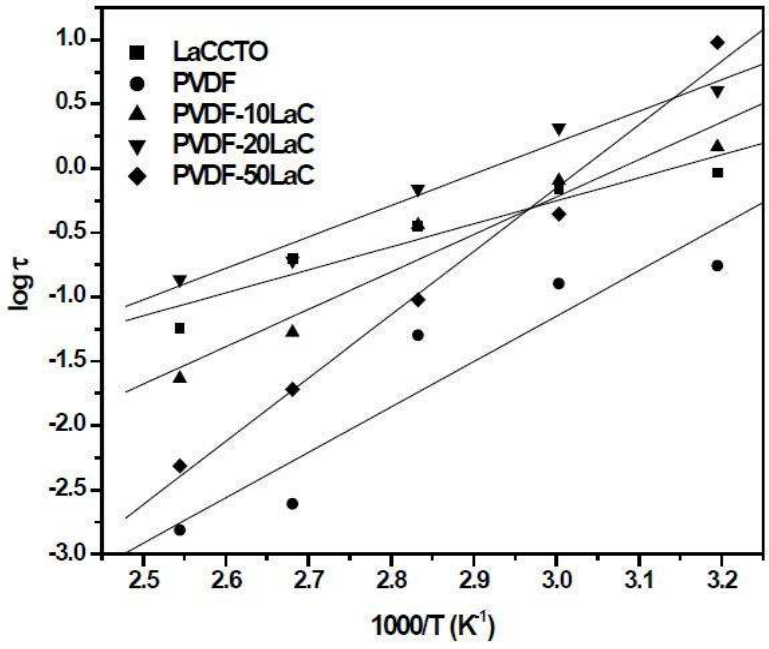

Figure 5.7 Log τ vs 1000/T plot for LaCCTO, PVDF, PVDF-10LaC, PVDF-20LaC and PVDF-50LaC.

Table 5.1 Activation energy of dielectric relaxation, α_c, relaxation associated with molecular motion of the polymer chains in the crystalline regions of PVDF from M'' vs log f plots.

Sample	Activation Energy
LaCCTO	**0.35 eV**
PVDF	**0.70 eV**
PVDF-10LaC	**0.72 eV**
PVDF-20LaC	**0.73 eV**
PVDF-50LaC	**0.98 eV**

It is also noted from Fig 5.6 (c) M'' peaks shift to low frequency with increasing content of LaCCTO. This is also because of the restricted movement of the polymer chains as mentioned above. It is also in conformity with the increasing value of Young's modulus with increase in the content of LaCCTO as described in section 5.4.

The effective dielectric permittivity (ε' or ε_{eff} are the same) of the composites can be calculated by various models reported in the literature. The dielectric property of a biphasic dielectric mixture comprising of spherical crystallites with high dielectric permittivity in a matrix of low dielectric permittivity can be described by Maxwell's model [Maxwell 1954]. According to this model, the effective dielectric permittivity of the composite is given by

$$\varepsilon_{eff} = \frac{\delta_p \, \varepsilon_p \left(2/3 + \varepsilon_c/3\varepsilon_p\right) + \delta_c \, \varepsilon_c}{\delta_p \left(2/3 + \varepsilon_c/3\varepsilon_p\right) + \delta_c} \qquad (5.3)$$

where ε_c, ε_p, δ_c and δ_p are the dielectric permittivity of LaCCTO, PVDF, the volume fraction of the ceramic and the polymer respectively. After substituting the values of ε_c, ε_p, δ_c and δ_p, the values of ε_{eff} obtained deviate much from the experimental values for all the volume fractions of LaCCTO under study (Fig 5.8).

In the case of Clausius-Mossotti model [Frolich 1949], it is assumed that the mixture of dielectric is composed of spherical crystallites dispersed in a continuous medium. The effective dielectric permittivity (ε_{eff}) of the composite is given by the following equation.

$$\varepsilon_{eff} = \varepsilon_p \left[1 + 3\delta \left(\frac{(\varepsilon_c - \varepsilon_p)}{\varepsilon_c + 2\varepsilon_p}\right)\right] \qquad (5.4)$$

The predicted value of ε_{eff} using this model also deviates a lot from the experimental values (Fig 5.8).

Lichtenecker's or logarithmic mixture rule is used to predict the effective dielectric permittivity value [Nalwa 1995]. According to this model ε_{eff} is given by

$$\text{Log } \varepsilon_{eff} = \delta_1 log\varepsilon_1 + \delta_2 log\varepsilon_2 \qquad (5.5)$$

Experimental results are significantly different from the predicted results using this model also (Fig 5.8). This is because Logarithmic law is applicable only when there is not much difference in the value of ε' of the dispersion medium and the dispersed phase. This is not true in the case of PVDF-LaC composites. ε' of LaCCTO is far greater than ε' of PVDF. Therefore the experimental results do not match exactly with the values predicted by this model.

The effective medium theory (EMT) model [Rao et al (2000] has been developed taking into account the morphology of the particles. According to this model, the ε_{eff} is given by

$$\varepsilon_{eff} = \varepsilon_p \left[1 + \frac{f_c(\varepsilon_c - \varepsilon_p)}{\varepsilon_p + n(1 - f_c)(\varepsilon_c - \varepsilon_p)}\right] \qquad (5.6)$$

where f_c is the volume fraction of the ceramic dispersed, ε_c, ε_p and *n* are the dielectric permittivity of the ceramic, polymer and the ceramic morphology fitting factor respectively. The experimental values obtained are closest to the predicted values in this case of all the models employed to predict the ε_{eff} values. The shape parameter n has been found to be 0.091.

All these models have the limitations that the chemistry of interfacial structure has not been taken into account and particles are assumed to be of spherical shape. Microstructure and microchemistry of the interfaces are also very important to determine the physical, mechanical and electrical properties of the composites.

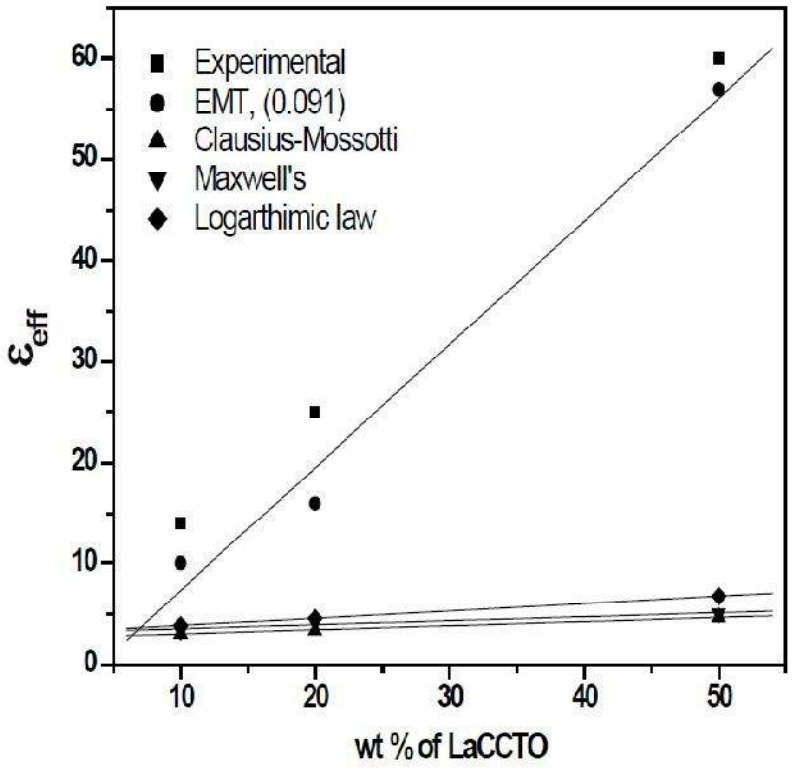

Figure 5.8 Variation of effective dielectric permittivity (ε_{eff}) measured at 100 Hz and 40^{o}C for PVDF-LaC composites based on various models.

Temperature-dependence of dielectric relaxation is explained by Havriliak-Negami (H-N) function [Windlass et al (2001); Mijovic et al (2006)]:

$$\varepsilon^{*} = -i\frac{\sigma_{dc}}{\varepsilon_0 \omega^{s}} + \varepsilon_{\infty} + \sum_{j}\frac{(\Delta\varepsilon)_j}{[1+(iw\tau_j)^{\alpha}]^{\beta}} \qquad (5.7)$$

where, σ_{dc} is dc conductivity, ω is the angular frequency, s is an exponent ($0<s \leq 1$), τ_j is the relaxation time of the j^{th} process, ε_0 is the vacuum permittivity, $\Delta\varepsilon$ is the dielectric strength of the j^{th} process and α and β are the shape parameters of the H-N function which define the symmetric and asymmetric broadening of the α_c relaxation peak in ε'' curve. Analysis of H-N function using WinFit software program of PVDF and PVDF-50LaC composite have been given in Table 5.2 using deconvoluted H-N fits presented in (Fig.5.9). The exponent parameter, α represents the slope of the lower frequency side of the relaxation peak in ε'' curve. β is the asymmetry parameter which is calculated from the slope of the higher frequency side of the same curve as α. The higher value of α for the composites as compared to pure PVDF indicates a stretched (broad) relaxation over a wider range of frequencies whereas $0<\beta\leq1$ represents asymmetrical broadening for the relaxation function. For $\beta=1$, the Debye-function is obtained. Asymmetry parameter β has a value of 1 for PVDF showing the symmetry of the spectrum. For the composites, β parameter has different values due to the dispersion of ceramics particles which creates heterogeneity in the system. For the composites, the relaxation time (s) calculated from H-N fit decreases with increase in temperature. The composites exhibit lower relaxation time as compared to PVDF. With increase in the temperature, the relaxation time decreases in the composites. Lower value of relaxation time at higher temperature is because of the ease of relaxation at higher temperature due to increased mobility of the chains both for pure PVDF as well as the composites.

Table 5.2 Fitting parameters for α_c relaxation as a function of temperature obtained from H-N fits.

Temp	PVDF, α	PVDF-50LaC, α	PVDF, β	PVDF-50LaC, β	PVDF, τ	PVDF-50LaC, τ
40^0C	0.49	0.60	1	0.57	2.33E-2	4.32E-3
80^0C	0.53	0.64	1	0.62	1.45E-3	8.26E-4
120^0C	0.57	0.77	1	0.72	7.44E-4	3.18E-5

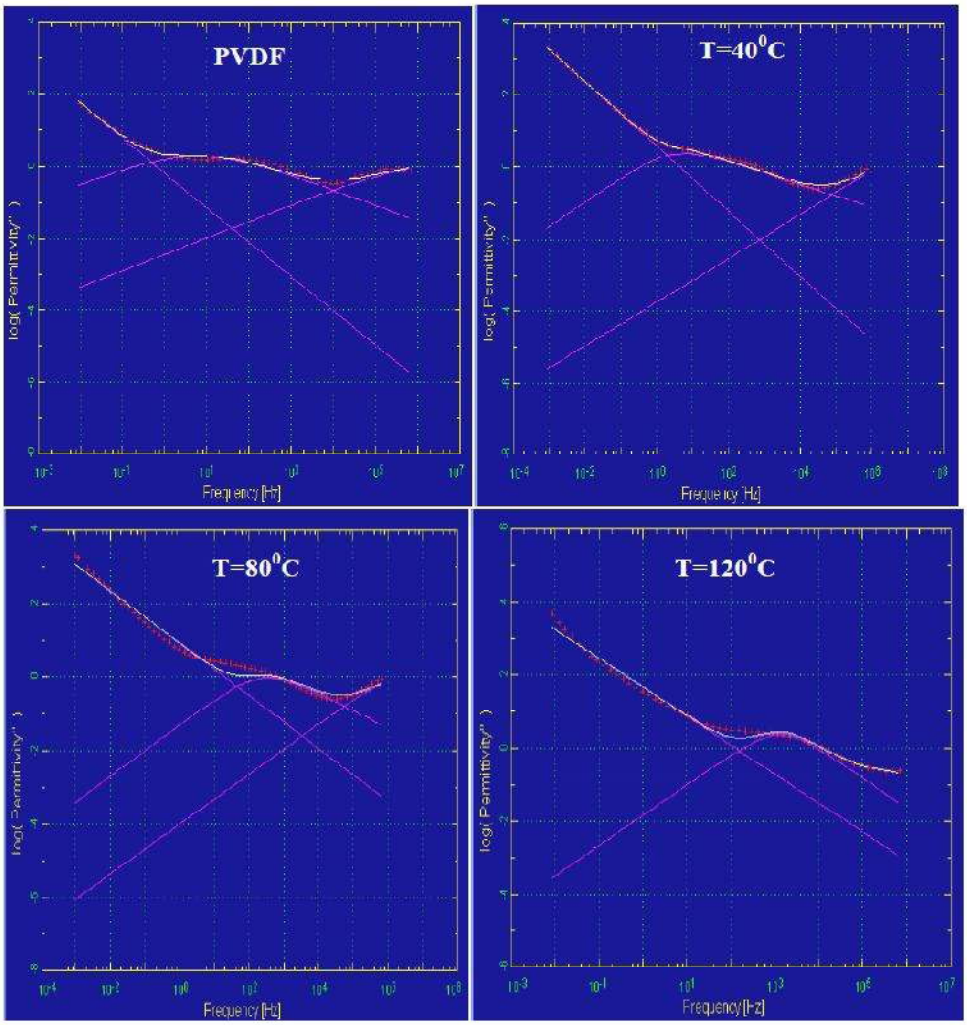

Figure 5.9 Dielectric loss in the frequency domain and spectrum was deconvoluted from H-N fits for PVDF-50LaC composites at different temperatures.

5.6. Conclusion

- Composites containing 10, 20 and 50 wt % LaCCTO in PVDF have been prepared through melt extrusion process.

- XRD studies indicate that there is no change of structure of either the polymer or ceramic in the composites but d-spacing is more in LaCCTO as compared to CCTO suggesting better interaction between PVDF and LaCCTO.

- Young's modulus increases significantly with presence of ceramic filler.

- Morphological studies reveal the homogeneous distribution of LaCCTO fillers in PVDF matrix.

- With addition of LaCCTO, there is substantial increase in the dielectric permittivity of the matrix PVDF. Dielectric loss increases slightly with increasing temperature and decreases with increasing frequency. Composites exhibit two dielectric relaxations and the relaxation peaks shift towards higher frequency with increasing temperature.

- As the filler content increases in the PVDF matrix, M' value decreases. In the modulus spectroscopy two dielectric relaxations have been observed in the composites. One relaxation occurring at low frequency is of Maxwell-Wagner-Sillar (MWS) type, while the other relaxation occurring in the intermediate frequency range is due to α_c relaxation associated with molecular motion of the polymer chains in the crystalline regions of PVDF.

- Temperature dependent dielectric relaxation has been worked out in details through H-N function. Debye type relaxation is observed in pure PVDF with $\beta=1$, while stretched relaxation over a wider range of frequency has been observed in the composites suggesting asymmetric nature of the relaxation.